Scientia Pharmaceutica

ÖSTERREICHISCHE PHARMAZEUTISCHE GESELLSCHAFT

MDPI

Article

Effect of Edge Activator Combinations in Transethosomal Formulations for Skin Delivery of Thymoquinone via Langmuir Technique

Hana Mohd [1,2], Katarzyna Dopierała [3], Anze Zidar [4], Amitkumar Virani [1,2] and Bozena Michniak-Kohn [1,2,*]

[1] Ernest Mario School of Pharmacy, Rutgers-The State University of New Jersey, 160 Frelinghuysen Road, Piscataway, NJ 08854, USA; hm527@dls.rutgers.edu (H.M.); amv160@scarletmail.rutgers.edu (A.V.)
[2] Center for Dermal Research, Rutgers-The State University of New Jersey, 145 Bevier Road, Piscataway, NJ 08854, USA
[3] Institute of Chemical Technology and Engineering, Poznan University of Technology, Berdychowo 4, 60-965 Poznan, Poland; katarzyna.dopierala@put.poznan.pl
[4] Department of Pharmaceutical Technology, Faculty of Pharmacy, University of Ljubljana, Aškerčeva Cesta 7, 1000 Ljubljana, Slovenia; anze.zidar@ffa.uni-lj.si
* Correspondence: michniak@pharmacy.rutgers.edu

Abstract: Thymoquinone (TQ), a bioactive compound found in *Nigella sativa* seeds, possesses diverse therapeutic properties for skin conditions. However, formulating TQ presents challenges due to its hydrophobic nature and chemical instability, which hinder its skin penetration. Transethosomes, as a formulation, offer an environment conducive to enhancing TQ's solubility, stability, and skin permeation. To optimize TQ transethosomal formulations, we introduced a combination of ionic and nonionic surfactants, namely Tween 20 and sodium lauryl sulfate (SLS) or sodium lauroyl glutamate (SLG). Surfactants play a crucial role in stabilizing the formulation, reducing aggregation, improving biocompatibility, and minimizing potential toxicity. We fine-tuned the formulation composition and gained insights into its interfacial behavior using the Langmuir monolayer technique. This method elucidated the interfacial properties and behavior of phospholipids in ethosome and transethosome formulations. Our findings suggest that monolayer studies can serve as the initial step in selecting surfactants for nanocarrier formulations based on their interfacial dilational rheology studies. It was found that the addition of surfactant to the formulation increased the elasticity considering the capability of transethosomes to significantly decrease their radius when permeating the skin barrier. The results of the dilational rheology experiments were most relevant to drug permeation through the skin for the largest amplitude of deformation. The combination of Tween 20 and SLS efficiently modified the rheological behavior of lipids, increasing their elasticity. This conclusion was supported by in vitro studies, where formulation F2 composed of Tween 20 and SLS demonstrated the highest permeation after 24 h (300.23 μg/cm^2). Furthermore, the F2 formulation showed the highest encapsulation efficiency (EE) of 94%, surpassing those of the control and ethosomal formulations. Additionally, this transethosomal formulation exhibited antimicrobial activity against *S. aureus*, with a zone of inhibition of 26.4 ± 0.3 mm. Importantly, we assessed the cytotoxicity of both ethosomes and transethosomes at concentrations ranging from 3.5 μM to 50 μM on HaCaT cell lines and found no cytotoxic effects compared to TQ hydroethanolic solution. These results suggest the potential safety and efficacy of TQ transethosomal formulations.

Keywords: thymoquinone; transethosomes; ethosomes; Langmuir study; transdermal

check for updates

Citation: Mohd, H.; Dopierała, K.; Zidar, A.; Virani, A.; Michniak-Kohn, B. Effect of Edge Activator Combinations in Transethosomal Formulations for Skin Delivery of Thymoquinone via Langmuir Technique. *Sci. Pharm.* **2024**, *92*, 29. https://doi.org/10.3390/scipharm92020029

Academic Editor: Natasa Skalko-Basnet

Received: 17 April 2024
Revised: 19 May 2024
Accepted: 23 May 2024
Published: 27 May 2024

Copyright: © 2024 by the authors. Licensee MDPI, Basel, Switzerland. This article is an open access article distributed under the terms and conditions of the Creative Commons Attribution (CC BY) license (https://creativecommons.org/licenses/by/4.0/).

1. Introduction

Thymoquinone (TQ), 2-Methyl-5-(propan-2-yl) cyclohexa-2,5-diene-1,4-dione, is the main bioactive component of the volatile oil of Nigella sativa seeds [1]. It has been used in conventional medicine as an antioxidant, antimicrobial, anti-inflammatory, and anticancer agent [2–6]. For example, TQ has shown potential for treating acne vulgaris,

pigmentation, vitiligo, hypersensitivity reactions, psoriasis, and even the early stages of skin tumorigenesis [7–9]. Most of these beneficial health effects can be attributed to the free radical-scavenging effects of TQ and the induction of antioxidant enzymes [10,11]. However, the clinical utilization of TQ is limited by its high hydrophobicity and chemical instability, which lead to poor bioavailability. Currently, thymoquinone (TQ) lacks FDA approval for therapeutic use. Nevertheless, numerous research efforts are underway to formulate TQ in various dosage forms, to overcome its solubility and stability challenges. This is especially evident in dermal applications, where the specific physicochemical characteristics limit TQ's ability to effectively penetrate the stratum corneum and reach the affected layers of the skin [12,13]. Therefore, it is considered an appealing approach to develop effective delivery systems that can enhance TQ's solubility and drug stability and facilitate its penetration and retention in the skin [14].

Vesicular systems such as ethosomes and transethosomes could prove to be effective delivery systems for TQ because of their ability to improve drug solubility and enhance the therapeutic concentration at the target site. Ethosomal formulations comprise phospholipids, ethanol, and water [15–17]. They have many advantages over traditional liposomes, including enhanced drug solubility, a higher loading capacity, and high deformability, which facilitate penetration through the stratum corneum into deeper skin layers [18]. Ethosomes have demonstrated enhanced drug entrapment, skin penetration, and deposition of various drugs [19–21]. Transethosomes are an advanced version of ethosomes owing to the addition of edge activators in comparison to the original ethosomes [22].

Edge activators include nonionic, ionic, or cationic surfactants. Nonionic surfactants, such as Tween 20, contribute to steric stabilization by forming a protective layer on the particle surface, which prevents interactions between vesicles [23]. Ionic surfactants such as sodium lauryl sulfate (SLS) provide electrostatic stabilization by creating a charged layer around nanoparticles, thereby reducing their aggregation [24,25]. Sodium lauroyl glutamate (SLG) is an ionic surfactant derived from the amino acids glutamic acid and lauric acid [26]. The addition of nonionic surfactants to ionic surfactants can improve biocompatibility and reduce potential cytotoxicity compared to the use of ionic surfactants alone [27]. Therefore, we propose the combination of a nonionic surfactant with an ionic surfactant: Tween 20 combined with sodium lauryl sulfate (SLS) or sodium lauryl glutamate (SLG).

To optimize the composition of these formulations, we employed the Langmuir monolayer technique, which clarifies the interfacial properties and behavior of phospholipids in ethosome and transethosome formulations [28,29]. This study provides valuable insights into film-forming characteristics and enables the optimization of formulation parameters for improved drug delivery through the skin [30].

This study aimed to explore the application of transethosomes as a promising carrier system for facilitating the transdermal administration of thymoquinone. Specifically, we examined the effects of combining ionic and nonionic surfactants on the performance of a transethosomal formulation using the Langmuir method to achieve the most effective transdermal delivery system while ensuring an acceptable safety profile.

2. Materials and Methods

2.1. Materials

Phospholipon 90G was provided by LIPOID LLC (Newark, NJ, USA). Tween 20 and sodium lauroyl glutamate were purchased from Sigma-Aldrich and Santa Cruz Biotechnology, respectively. Ethanol 200 proof was purchased from Sigma-Aldrich (St. Louis, MO, USA). Thymoquinone analytical standard was purchased from sigma-Aldrich. This study utilized HPLC-grade water and chloroform obtained from Sigma-Aldrich, as well as HPLC-grade acetonitrile from Midland Scientific (Omaha, NE, USA). Dermatomed human cadaver skin was procured from The New York Firefighters Skin Bank. The donor was a 74-year-old male weighing 118 lb (New York, NY, USA). The remaining chemicals utilized in the research were of reagent quality and procured from VWR International (Radnor, PA, USA).

2.2. Methods

2.2.1. Monolayer Study

The experiment was performed using a Langmuir trough (Biolin Scientific, Stockholm, Sweden) with a surface area of 98 cm^2 equipped with symmetrical, hydrophilic barriers and a platinum Wilhelmy plate. Phosphate-buffered saline (PBS) was used as the subphase. The lipids were dissolved in chloroform and carefully spread on the subphase using a syringe. After the solvent evaporated, the monolayer was compressed using two symmetrical movable barriers. Simultaneously, the mean molecular area (A) and surface pressure (π) were recorded. For the investigation of lipid–surfactant interactions, the soluble surfactants (Tween 20, sodium lauryl sulfate (SLS), sodium lauroyl glutamate (SLG), Tween 20 + SLS, or Tween 20 + SLG) were dissolved in PBS to a concentration of 0.84 μg/mL, and 10 μL of the solution was introduced to the subphase before spreading the lipid. The final concentration of the surfactant in the subphase was 2.15 ng/mL. The data from the π-A isotherms were used to calculate the compression modulus (C_s^{-1}) according to Equation (1):

$$C_s^{-1} = -A\left(\frac{\Delta \Pi}{\Delta A}\right)_T \quad (1)$$

The lower the value of C_s^{-1}, the more compressible is the monolayer. Dilational rheology experiments were performed using the oscillating barrier method. After the monolayer was compressed to π = 30 mN/m, a sinusoidal area deformation was applied using a frequency (ω) of 10 mHz and an amplitude of 1–20%. Based on the surface pressure response to area deformation, the dilational modulus (G) was obtained, which is a complex quantity composed of a real component (G') and an imaginary component (G'') representing the elastic and viscous behaviors, respectively. For a perfectly elastic response, the imaginary part is zero, whereas for a perfectly viscous film, the real part is zero. Most films of biological relevance are viscoelastic, exhibiting intermediate properties between purely elastic and purely viscous films. The values of G' and G'' were determined based on 3 independent experiments, and each experiment was performed as 3 full oscillation cycles. All monolayer experiments were performed at 20 °C.

2.2.2. Preparation of Ethosome and Transethosome Formulations with Thymoquinone

TQ and Phospholipon 90G, with or without an edge activator (SLS, Tween 20, and SLG), were dissolved in ethanol, in a sealed glass bottle. The mixture was stirred using a magnetic stirrer at 700 rpm with heating at 30 °C for 30 min. PBS was heated to 30 °C and then slowly added at a constant rate of 200 μL/min until reaching a final volume of 100% (w/w) (as shown in Table 1). After the PBS was added, stirring was continued for an additional 5 min [31]. The mixed solution was then placed in an ultrasonic apparatus and subjected to two cycles with a total of 10 min each of probe sonication (SFX Branson Ultrasonic Processor, Emerson Industrial Automation, St. Louis, MO, USA) in pulse mode with 2 min intervals between the cycles. The control formula was prepared by dissolving 200 mg of TQ in 100 mL hydroethanolic solution (50% ethanol).

Table 1. The compositions of the formulations investigated in this study.

Formula	TQ (% *w*/*w*)	Tween 20 (% *w*/*w*)	SLS (% *w*/*w*)	SLG (% *w*/*w*)	Ethanol (% *w*/*w*)	Ph90 (% *w*/*w*)	PBS
F1	0.2	0.5	-	-	50	3	q.s.
F2	0.2	0.4	0.1	-	50	3	q.s.
F3	0.2	0.4	-	0.1	50	3	q.s.
E	0.2	-	-	-	50	3	q.s.

TQ: thymoquinone, SLS: sodium lauryl sulfate, SLG: sodium lauryl glutamate, Ph90: Phospholipon 90G, PBS: phosphate-buffered saline, q.s.: quantity sufficient.

2.2.3. Characterization of Ethosomes and Transethosomes

The ethosome and transethosome formulations were assessed for their average vesicle size and size distribution (polydispersity index, PDI) using Dynamic Light Scattering (DLS) (Zetasizer Nano-S, Malvern Panalytical, Westborough, MA, USA). The zeta potential was measured by Electrophoretic Light Scattering (ELS) (Zetasizer Nano series, Malvern Panalytical). All formulation samples were analyzed at room temperature without additional processing.

2.2.4. Entrapment Efficiency (EE)

The EE was determined by ultrafiltration of a sample through Centrisart 10 kDa MWCO, centrifugation at 40,000 rpm for 20 min, and subsequent analysis of the filtrate using the HPLC method described in Section 2.2.5 below. The percentage of drug entrapment was calculated using Equation (2):

$$D_{EE} = \left(\frac{D_t - D_s}{D_t} \right) \times 100 \quad (2)$$

where Dt is the total amount of drug added and Ds is the amount of drug obtained in the filtrate [32,33].

2.2.5. High-Performance Liquid Chromatography (HPLC)

High-performance liquid chromatography (HPLC) was performed using the Agilent 1100 Series HPLC system (Agilent Technologies, Santa Clara, CA, USA). The instrument was coupled with a UV diode array detector (DAD) and operated using HP Chemstation software V. 32. The composition of the mobile phase comprised 80% acetonitrile and 20% water. To assess the quantity of TQ, a mobile phase was pumped at a flow rate of 1.0 mL/min through an Agilent Eclipse XDB-C18 column of dimensions 250 mm length × 4.6 mm internal diameter, with 5.0 µm vesicle sizes as the stationary phase at 25 °C. The sample injection size was 20 µL. The column temperature was maintained at 23 °C, and UV detection of TQ was performed at a wavelength of 250 nm; the retention time of TQ was 3.4 min [34]. The linearity of the peak area versus concentration was evaluated using a standard concentration range from 0.39 µg/mL to 100 µg/mL, yielding a coefficient of regression (R^2) of 0.99. The method demonstrated precision, with a % RSD (relative standard deviation) of 0.13% for intra-day measurements and 0.86% for inter-day measurements. The limit of detection (LOD) was determined to be 0.54 ng/mL, whereas the limit of quantification (LOQ) was 1.64 ng/mL.

2.2.6. In Vitro Skin Permeation Study

To assess the permeation of TQ, full-thickness dermatomed human cadaver skin obtained from the posterior torso was obtained from the New York Firefighters Skin Bank (USA). Upon arrival, the skin was immediately frozen at a temperature of −80 °C. On the day of the study, the skin was thawed in filtered phosphate-buffered saline (PBS, pH 7.4) at room temperature for 10 min. A suitable portion of the skin was then cut and positioned between the donor and receptor chambers of a vertical Franz diffusion cell (FDC), with the stratum corneum facing the donor chamber and the dermis part of the skin in contact with the receptor compartment. The receptor chamber was filled with a known volume of pH 7.4 PBS buffer and continuously stirred using a small polytetrafluoroethylene (PTFE)-coated magnetic bar rotating at 600 rpm. The skin surface temperature was maintained at 32 °C by placing the FDC in a dry block heater (Logan Instruments, Somerset, NJ, USA) set at a precise temperature of 37 ± 0.5 °C. Five Franz cells were used for the experimental group, with N = 5.

After the assembled FDCs were allowed to equilibrate for a minimum of 30 min, 500 µL of each formulation was applied to the skin in the donor compartment as described by Virani et al. [35,36]. At specific time intervals, a 300 µL sample of the receptor medium was withdrawn, and an equivalent volume of fresh buffer solution was added to the receptor

chamber. The corrected concentration of TQ in the withdrawn sample was analyzed using the HPLC method described in Section 2.2.5.

The effect of the formulation on skin integrity was investigated by conducting TEWL measurements before applying the formulation to the donor side and at the conclusion of the study, following established protocols [37].

The cumulative amount of permeated TQ per unit area was calculated using Equation (3):

$$Q_n = \frac{C_n V_r + \sum_{i=0}^{n-1} C_i V_s}{A} \quad (3)$$

where Q_n is the cumulative amount of the drug permeated per unit area (μg/cm^2) at different sampling times, C_n is the drug concentration in the receiving medium at different sampling times (μg/mL), C_i is the drug concentration in the receiving medium at sampling time i (n−1) (μg/mL), V_r is the volume of the receptor solution (mL), V_s is the volume of the sample withdrawn (mL), and A is the effective permeation area of the diffusion cell (cm^2). The Qn values were plotted over time, and the steady-state flux (Jss) was determined by analyzing the slope of the linear segment within the plot.

The permeability coefficient (K_p) was calculated with Equation (4):

$$K_p = \frac{J_{ss}}{C_0} \quad (4)$$

where J_{ss} is the steady-state flux (μg cm^{-2}h^{-1}), and C_0 is the concentration of TQ in the donor compartment (μg mL^{-1}).

The enhancement ratio was calculated by dividing the flux of the test formulation by that of the control formulation, which was TQ in hydroethanolic solution (TQ C), using Equation (5):

$$Enhancment\ ratio = \frac{J_{ss} \text{ of TQ in formulation}}{J_{ss} \text{ of TQ C}} \quad (5)$$

2.2.7. Skin Deposition Study

Upon completion of the permeation study, skin samples were extracted from the Franz diffusion cells. They were then carefully cut around the diffusion area, and the dermal and epidermal layers were separated manually with tweezers, allowed to air-dry, precisely weighed, and subsequently transferred into BeadBug tubes. To isolate the drug, skin samples were cut into small pieces using scissors. Subsequently, 1 mL of ethanol was added to each sample tube to facilitate the extraction from the skin [38]. The skin samples were homogenized using a BeadBug^{TM} Microtube homogenizer, D1030 (Benchmark Scientific, Sayreville, NJ, USA). Finally, samples were centrifuged at 1200 rpm for 5 min and filtered through a 0.45 μm polypropylene filter to remove skin debris. The filtered samples were analyzed using validated HPLC. The amount of TQ in the skin was represented as TQ (μg) per skin weight (mg).

2.2.8. Antimicrobial Assay

We used the disc diffusion method to test the antimicrobial activity of the TQ-loaded films against *S. aureus* (ATCC, Stock # 49230). Briefly, Muller Hinton agar (MHA) plates were prepared by pouring molten medium into sterile Petri dishes. Then, 100 μL of overnight cultured bacteria adjusted to an optical density (OD) concentration of 0.542 (OD 1 = 1 × 10^9/mL of bacteria) in sterile TSB (Tryptic Soy Broth) was spread on the surface of the MHA agar plates with the help of a sterile spreader. Subsequently, disc-shaped polymer films measuring 0.64 cm^2 and 100 μL of 40 μg TQ formulations were placed on the agar surface. The plates were then incubated at 37 °C for 24 h. As a positive control, azithromycin (99.0%, Sigma Aldrich, expiration date 31 December 2024) at a concentration of 15 μg/100 μL was employed, while the blank formulation served as a

negative control. After the incubation period, the inhibition zones surrounding the polymer discs were examined.

2.2.9. Cytotoxicity Assay

The cytocompatibility of TQ-loaded ethosomes and transethosomes was assessed on the HaCaT cell line (human keratinocytes, AddexBio) using AlamarBlue® assay. The cells were seeded into a 96-well flat-bottom plate at a density of 10,000 cells per well in 80 µL 1% FBS DMEM dispersion overnight. Then, 20 µL of TQ solution was added and incubated for 24 h. Cells treated with formulation-free media were included as a negative control. Then, 10 µL of AlamarBlue® was added and incubated for 3 h. The intensity of fluorescence was measured at 540 nm excitation and 560 nm emission using a microplate reader (Tecan, Männedorf, Switzerland).

2.2.10. Statistical Analysis

All results are reported as the mean ± SD (N = 5). Statistical analysis of the data was performed using one-way analysis of variance and Dunnett's multiple comparison test. Statistical significance was set at $p < 0.05$.

3. Results and Discussion

3.1. A Monolayer Study

The π-A isotherms for Ph90 in the presence of various surfactants are shown in Figure 1a. Except for SLS, the surfactants caused a significant shift in the curves towards higher-molecular-weight areas, indicating their insertion into the lipid monolayer. Similar results were reported for lipid monolayers in the presence of other soluble surfactants such as 1-alkyl-1-methylpiperidinium bromides [39]. Other authors suggested that cationic and anionic surfactants may affect lipid monolayers by different mechanisms governed by electrostatic forces [40]. The effect of soluble surfactants on phospholipid films is often explained via a kinetic barrier of desorption of the surfactant from the air/water interface, which is different for neutral and charged molecules [41]. Our results demonstrate the potential of surfactants to affect lipid monolayers and act as edge activators in pharmaceutical formulations based on Phospholipon 90. Furthermore, the elevated initial surface pressure at $A \approx 130$ Å^2/mole confirmed the surface activity of the surfactants and the synergistic effect of Tween 20 + SLG and Tween 20 + SLS, which increased the surface pressure more efficiently than the single surfactants alone did at the same total concentration. This implies that the functionalization of lipid vesicles might be achieved using a smaller total amount of edge activators if Tween 20 is mixed with an anionic surfactant, in comparison to a single surfactant. The monolayer of Ph90 was also slightly more stable in the presence of Tween 20 + SLG and Tween 20 + SLS as the monolayer collapsed at a higher surface pressure than was observed for the other films. This result indicates that the addition of these surfactants may have a slightly positive impact on the stability of transethosomes. The compression modulus curves in Figure 1b reflect the packing and ordering of the films. The plot indicates the fluidizing effects of Tween 20 and SLG on the lipid monolayer, as their maximum values of C_s^{-1} were lower than that of Ph90. This indicates that the monolayer is more compressible in the presence of these compounds, which might be perceived as beneficial for lipid vesicles that can more easily undergo deformation during transdermal drug delivery. By contrast, SLS increased the compression modulus, suggesting that the monolayer became more compact. The combination of surfactants caused fluidization of the monolayer only for <35 mN/m; however, the maximum C_s^{-1} value was reached at 39 mN/m, which was close to the value obtained for the Ph90 monolayer. This suggests that vesicles modified with combined surfactants may be more tightly packed, smaller, and less susceptible to drug leakage.

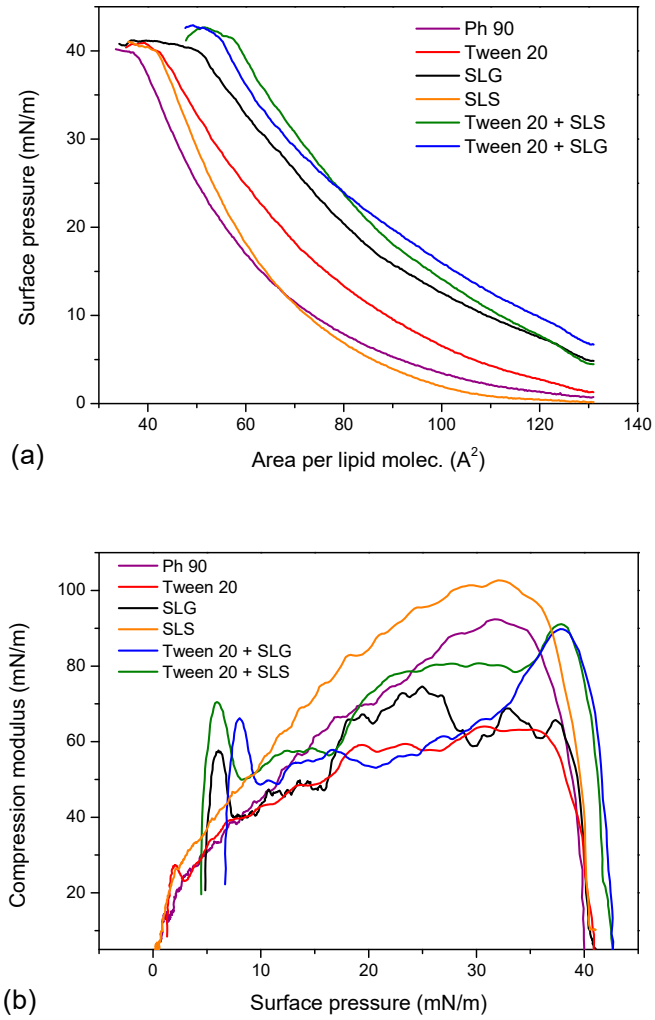


Figure 1. The π-A isotherms (**a**) and compression modulus curves calculated using Equation (1) (**b**) for Ph90 in the presence of various edge activators and their combinations in the subphase.

The results of the interfacial dilational rheology studies are shown in Figure 2 as average values with standard deviations. The dominance of elastic properties over viscous behavior was observed when comparing the G″ and G′ values for the same amplitude. Most of the surfactants caused an increase in G′ in comparison to the monolayer of pure Ph90. The largest effect was observed with Tween 20, SLS, and their combination, suggesting their considerable potential to modify the deformability of lipid nanocarriers in formulations and enhance the permeation of the drug through the skin. For SLG and Tween 20 + SLG, the elastic modulus was close to the G′ observed for pure Ph90, regardless of the amplitude applied. The contribution of the viscous component to the interfacial viscoelasticity was most significant for small amplitudes and decreased with increasing amplitude. Considering the capability of transethosomes to significantly decrease their radius when permeating the skin barrier, the results of the dilational rheology experiments were most relevant to drug permeation through the skin for the largest amplitude of deformation. Therefore, by analyzing the values of G′ for an amplitude of 20%, one can observe the positive impact of Tween 20, SLS, and their combination on the elastic response of the lipid layer on area deformation. This means that vesicles modified with these edge activators may be capable of restoring their original size and shape after the force-causing deformation is removed. In other words, these vesicles may be more flexible and stable than the other formulations.

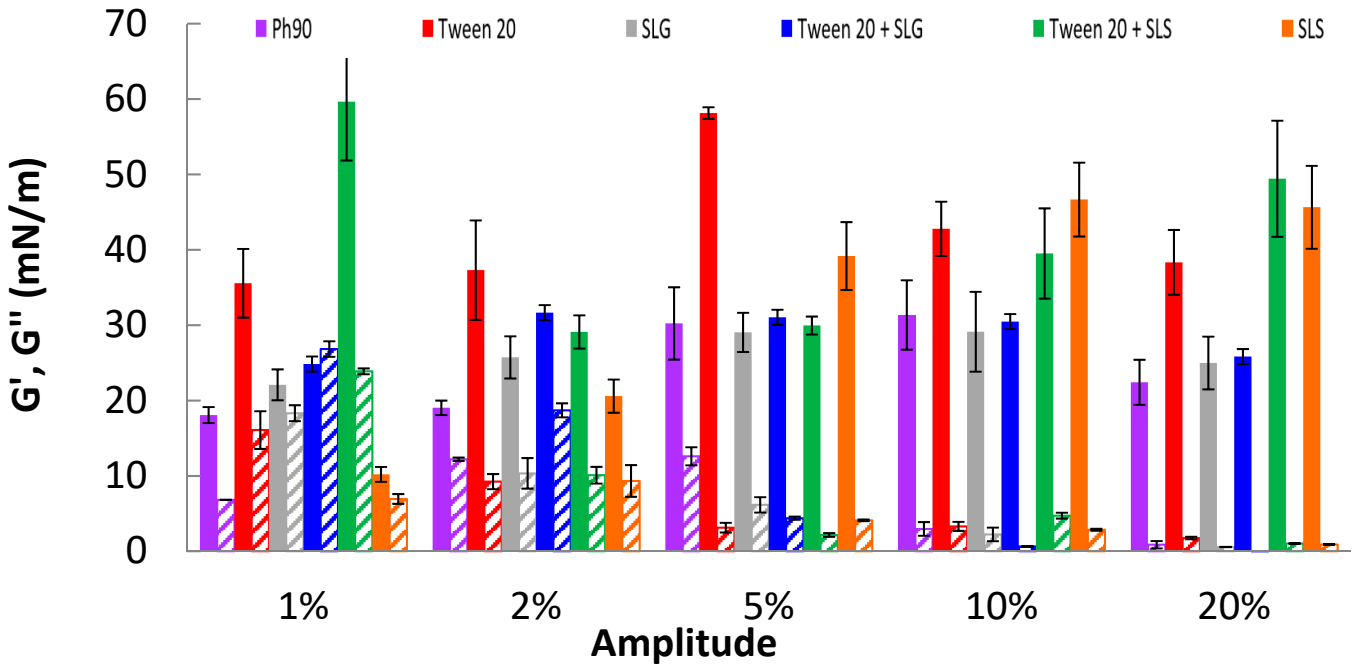


Figure 2. The elastic (G′, full bars) and viscous (G″, patterned bars) dilational moduli of the lipid film in the presence of surfactants determined for various amplitudes of oscillations.

Overall, the results of the monolayer study indicated that the role of edge activators in transethosomes is complex and includes several mechanisms that may lead to an increase in stability, changes in size, and an improvement in deformability. Therefore, all the surfactants used may improve the properties of the vesicles; however, the mechanism of their activity may be slightly different. The combinations of Tween 20 with SLS and SLG may be easily incorporated into the lipid vesicle; however, only Tween 20 + SLS efficiently modified the rheological behavior at high amplitudes, which is why this combination might be the most promising for enhancing drug transport through the skin.

3.2. Characterization of TQ-Loaded Ethosomes and Transethosomes and the Effect of Different Edge Activators

Characterization of the prepared TQ-loaded ethosomes and transethosomes is crucial to understand their permeability by considering factors such as their size, zeta potential, and encapsulated drug content. Hence, it is imperative to assess the vesicle size, polydispersity index (PDI), zeta potential, and %EE (Table 2) of TQ-loaded ethosomes and transethosomes.

Table 2. Physiochemical properties of the obtained vesicles. Data are presented as means ± SD (N = 3).

Formula Code	Zeta Average (nm)	PDI	EE%	Zeta Potential (mV)
F1	133.76 ± 1.26	0.20 ± 0.03	87% ± 0.34	−20 ± 0.3
F2	115.49 ± 0.72	0.19 ± 0.01	94% ± 0.26	−62 ± 0.4
F3	154.67 ± 2.68	0.22 ± 0.02	92% ± 0.35	−32 ± 0.6
E	164.14 ± 5.05	0.12 ± 0.02	81% ± 0.41	−38 ± 0.2

EE: entrapment efficiency, PDI: polydispersity index.

The results revealed that the type of surfactant played a significant role ($p < 0.05$) in determining the vesicle size.

Generally, the addition of an edge activator leads to a decrease in the vesicle size. Transethosomes prepared with a combination of Tween 20 and SLS exhibited the smallest

vesicle size (115.4 nm), followed by those prepared with Tween 20 alone (133.7 nm) and, finally, those prepared with a combination of Tween 20 and SLG-based transethosomes (154.3 nm).

Furthermore, the combination of nonionic and ionic surfactants has been shown to increase entrapment efficiency. The entrapment efficiency is influenced by the phase transition temperature (Tc) of the surfactant, with higher Tc values generally resulting in a higher entrapment efficiency. Additionally, the use of an embedded edge activator (surfactant) such as SLS, SLG, or Tween 20 can solubilize the drug in the lipid bilayer, contributing to a significant increase in the entrapment efficiency of the encapsulated drugs [42].

Anionic surfactants possess a negative charge, which allows them to interact with positively charged drug molecules via electrostatic interactions. This interaction promotes the entrapment of the drug within the vesicles, leading to increased entrapment efficiency. The anionic surfactant SLS enhances the repulsive force between the lipid bilayers, increasing membrane elasticity and enabling vesicles to accommodate higher amounts of the drug, as confirmed by several publications [42]. Anionic transethosomes have been reported to exhibit higher %EE values than cationic ones [43].

Transethosomes also demonstrated a significantly higher %EE for TQ than did ethosomes. This can be attributed to the solubilizing properties of the surfactant and the interactions between the surfactants, thymoquinone, and lipid bilayer.

3.3. Ex Vivo Skin Deposition and Permeation Study

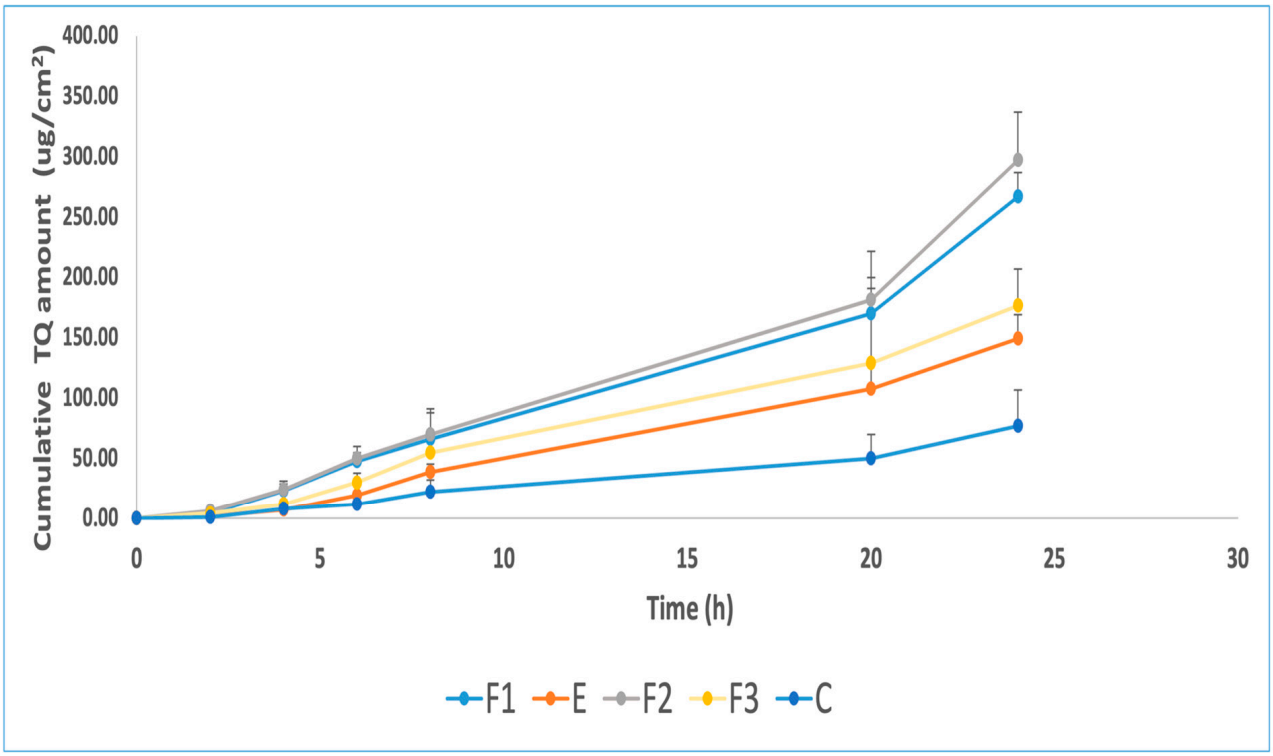
Ethosomes are a unique type of deformable lipid vesicle characterized by fluid lipid bilayers. They have been reported to enhance the delivery of various molecules into the deep skin layers. However, the precise mechanism underlying skin drug delivery by ethosomes is not fully understood [44]. High concentrations of ethanol in the formulation contribute to the flexibility of vesicles and evaporate from the formulation upon application to the skin surface under non-occlusive conditions [32]. However, the effect of the overall composition of ethosomes on the structure of the SC bilayer has not yet been completely elucidated. Nevertheless, their simple composition, the solubility-enhancing properties of ethanol for numerous drugs, and their ease of preparation make them promising candidates for the topical delivery of various drugs, particularly lipophilic drugs [45].

The presence of an embedded edge activator, in combination with ethanol, enhances the solubility of the drug and facilitates the formation of deformable lipid structures. These deformable ethosomes can easily traverse the skin corneocytes, thereby improving the retention and permeation of the drug in the skin [42].

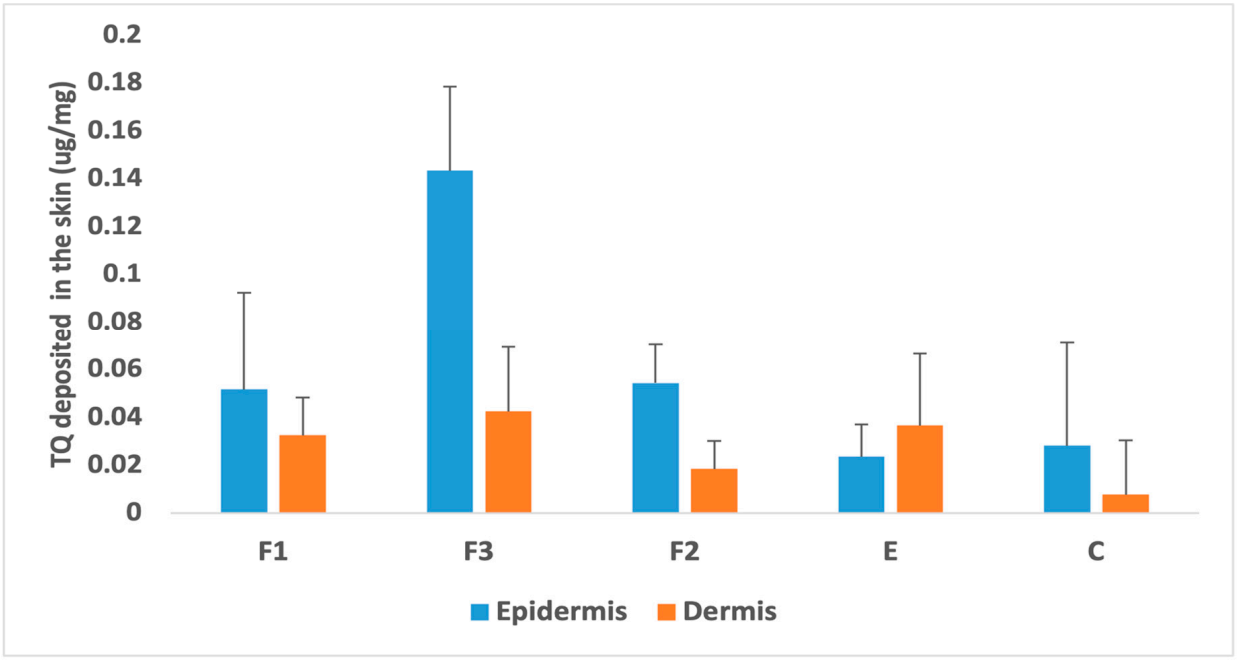
When developing a topical formulation, permeation and penetration studies are crucial because they provide insights into how the formulation behaves when it meets the skin, ultimately predicting its therapeutic effectiveness in vivo [46]. The skin barrier creates a hydrophobic environment, which is vital for the prevention and control of drug delivery [47].

TEWL measurements were conducted to assess skin integrity. The TEWL measurements, ranging from 1.4 to 12.4 $g \cdot m^{-2} \cdot h^{-1}$ before application, were considered acceptable. Moreover, no increase in TEWL was observed 24 h after application. This suggests that the application of the ethosomal and transethosomal formulations did not compromise the integrity of the skin barrier.

Ex vivo skin permeation experiments on human cadaver skin were performed using Franz diffusion cells to evaluate the potential of these formulations for TQ delivery through the skin. The drug permeation profiles of TQ, the cumulative amount of TQ that permeated through the epidermal and dermal layers over 24 h of the skin permeation study, and the amount of TQ deposited in the epidermal and dermal layers at 24 h after the completion of the skin permeation study are shown in Figure 3.



(**a**)



(**b**)

Figure 3. (**a**) Ex vivo drug permeation profiles of thymoquinone (TQ)-loaded ethosome and transethosome formulations over 24 h; (**b**) TQ deposited in the different layers of skin after a 24 h skin permeation study from the formulations tested (N = 5). Data are presented as means with SDs.

The permeation outcomes align closely with the findings of the monolayer study. Most surfactants notably increased the elasticity (G′) compared to that for the monolayer of pure lipids, with the largest effect from Tween 20, SLS, and their combination. This suggests their significant potential for altering the deformability of lipid nanocarriers within the formulation and thereby enhancing drug permeation through the skin. This potential was

particularly evident in the IVPT result for the F2 formulation, comprising SLS and Tween 20 in combination, which exhibited the highest permeation rate at 300.23 μg/cm^2 over 24 h. Similarly, F1 containing Tween 20 demonstrated considerable permeation at 276.42 μg/cm^2.

Moreover, the permeation results corroborate the observations from the monolayer study, where the elasticity (G′) in SLG + Tween 20 closely resembled that of the lipids alone. Values of 177.00 μg/cm^2 and 150.00 μg/cm^2 were observed for F3 and E, respectively, while the control exhibited a significantly lower value at 60 μg/cm^2. This observation justifies the higher skin deposition for the F3 formulation.

The enhanced permeation and deposition of TQ could be attributed to the presence of Tween 20 as an edge activator, along with SLS and GLS. In this study, Tween 20 was selected based on its favorable physicochemical characteristics, determined through Langmuir–Blodgett (LB) studies. The incorporation of Tween 20 and SLS as edge activators in TQ-deformable ethosomes resulted in higher entrapment efficiency and smaller vesicle size. Collectively, these factors contribute to the improved delivery of drugs to the skin.

The values of the steady-state flux (J_{ss}), permeability coefficient (Kp), and enhancement ratio are presented in Table 3.

Table 3. Permeation parameters obtained for the investigated formulations. Data are presented as means ± SD (N = 5), * $p < 0.01$ vs. control, # $p < 0.01$ vs. E.

Formulation	J_{ss} (μg cm^{-2} h $^{-1}$)	Kp (cm h^{-1})	Enhancement Ratio
Control	3.34 ± 0.90	0.003	-
F1	21.37 ± 0.01 *#	0.021	6.4
F2	23.71 ± 2.5 *#	0.037	9.8
F3	12.13 ± 1.8 *	0.013	3.63
E	11.71 ± 1.0 *	0.012	3.51

3.4. Antimicrobial Assay

Staphylococcus aureus is responsible for a significant proportion of skin, bone, deep tissue, and respiratory tract infections in humans. The emergence of antibiotic resistance in *S. aureus* highlights the critical need for novel approaches to treat these infections [48]. Hence, the antimicrobial effectiveness of the ethosomal and transethosomal formulations containing TQ was evaluated by determining the zones of *S. aureus* inhibition after 24 h in bacterial culture. The results and zones of inhibition are presented in Table 4 and Figure 4. Formulations loaded with TQ showed higher antibacterial activity than did those loaded with free TQ.

Table 4. Zones of inhibition of the tested formulations against *S. aureus*, N = 3.

Formulation	Zone of Inhibition (mm)
Azithromycin	7.82 ± 0.01
F1	10.0 ± 0.9
F2	26.4 ± 0.3
F3	18.1 ± 0.8
E	6.55 ± 0.9
TQ	1.8 ± 0.1
Blank formulation	0

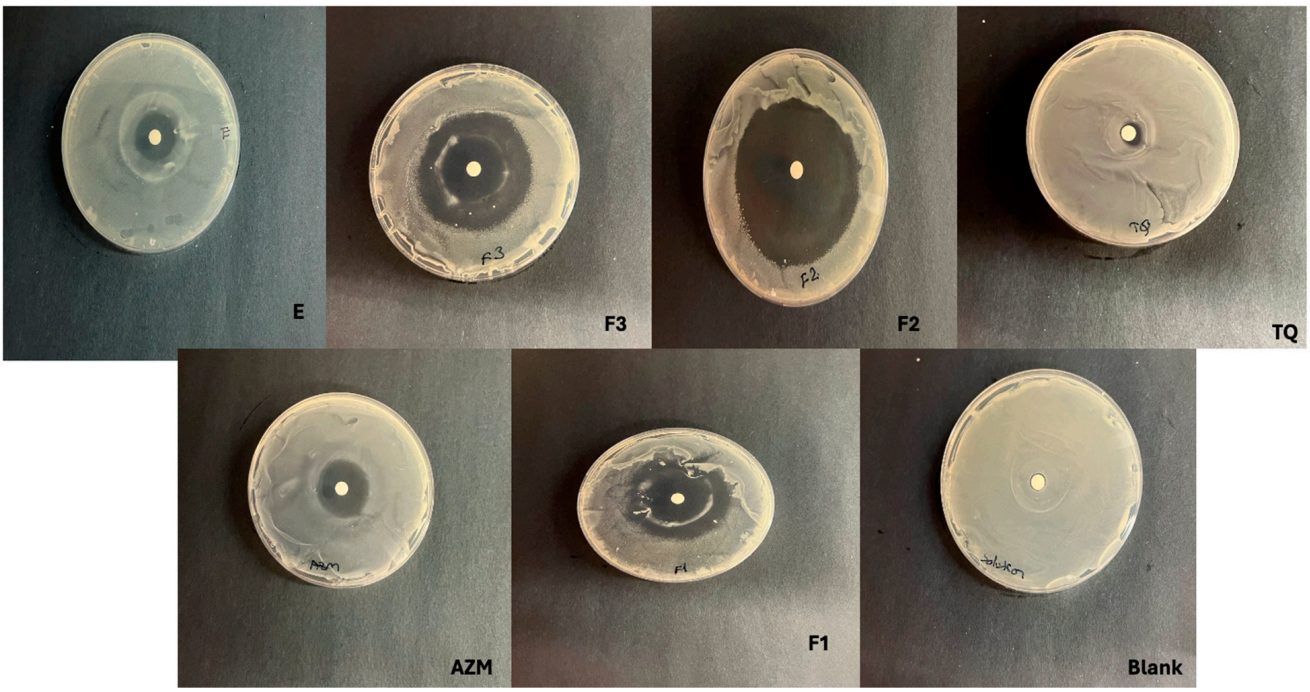


Figure 4. Bacterial inhibition study. Inhibition of *S. aureus* growth on agar plates by negative control; by azithromycin 15 μg, positive control; and by F1, F2, F3, E, and TQ 40 μg. AZM: azithromycin, TQ: the control formulation of TQ in hydroethanolic solution.

The transethosome formulation exhibited a stronger antimicrobial effect than did the ethosomal formulation or azithromycin. Neither the blank formulation nor the thymoquinone solution exhibited antimicrobial effects.

The enhanced antimicrobial effects of TQ delivered via transethosomes can be attributed to several factors. First, the smaller size of transethosomes compared to that of ethosomes allows for better penetration of the drug through the bacterial cell membrane, increasing its ability to disrupt the membrane and induce cell death. Secondly, transethosomes can protect the drug from degradation by enzymes, allowing a higher concentration of the active drug to be delivered to the site of action.

3.5. Cytotoxicity Study

To evaluate the safety of the transethosomal formulations, we performed a series of tests on the HaCaT human keratinocyte cell line. This study included the evaluation of three transethosomal formulations (F1–3), one blank formulation, and a single-component TQ solution. As shown in Figure 5, various concentrations of the formulations were examined, ranging from 3.125 to 50 μM TQ in the formulation or an equivalent amount of transethosomes in the blank formulation. The results indicated that the TQ formulations had a significantly improved safety profile compared to TQ alone. In addition, no discernible changes were observed among the three transethosomal formulations. These results highlight the potential of transethosomal delivery systems in improving the safety of TQ-based formulations for future applications.

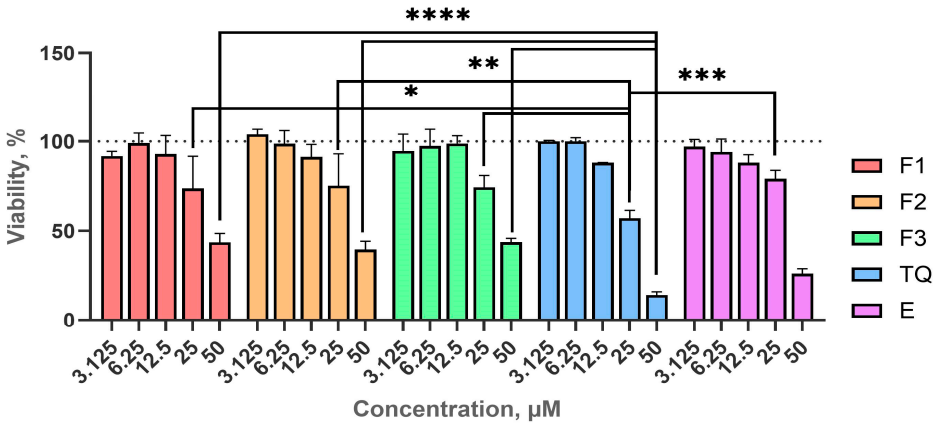


Figure 5. Viability of keratinocyte cell line (HaCaT) as measured by AlamarBlue assay after 24 hr of incubation with hydroethanolic TQ solution or TQ loaded in ethosomes or transethosomes. Data represent average values ± SD (N > 3). Statistically significant differences: * ($p < 0.05$), ** ($p < 0.01$), *** ($p < 0.001$), and **** ($p < 0.0001$).

4. Conclusions

Transethosomes emerge as superior skin delivery systems compared to ethosomes, particularly when formulated with a combination of edge activators. Our investigation, integrating Langmuir monolayer studies to elucidate interfacial behaviors, provides valuable insights into the mechanisms underlying the efficacy of transethosomal formulations and aids in formulation optimization, particularly in selecting the most suitable surfactant or combination thereof. Notably, the combination of Tween 20 and SLS yielded promising results by enhancing the elasticity of the lipid system and facilitating significant improvements in drug permeation through the skin barrier, as evidenced by its substantial enhancements in permeation, flux, encapsulation efficiency (EE), and antimicrobial activity against *S. aureus*. These findings underscore the potential of transethosomes as effective therapeutic agents for treating bacterial infections, while our cytotoxicity studies on human keratinocyte cells highlight the safety profile of transethosomal formulations compared to free TQ.

Author Contributions: Conceptualization, H.M. and B.M.-K.; methodology, H.M., K.D., A.Z., A.V. and B.M.-K.; software, H.M. and K.D.; validation, H.M. and A.Z.; formal analysis, H.M.; investigation, H.M. and B.M.-K.; resources, H.M. and B.M.-K.; data curation, H.M. and B.M.-K.; writing—original draft preparation, H.M., A.V. and B.M.-K.; writing—review and editing, H.M., A.V., K.D., A.Z. and B.M.-K.; visualization, H.M., A.Z., K.D. and A.V.; supervision, B.M.-K.; project administration, H.M. and K.D.; funding acquisition, B.M.-K. All authors have read and agreed to the published version of the manuscript.

Funding: This study was funded by the Center for Dermal Research CDR, Rutgers, The State University of New Jersey, 145, Bevier Road, Piscataway NJ 08854 and the European Union's Horizon 2020 Research and Innovation program under the Marie Skłodowska-Curie grant agreement No. 778051 (ORBIS project). Scientific work published within the international project was co-founded by the Ministry of Science and Education of Poland "PMW" in years 2019–2022 no. 5014/H2020—MSCA-RISE/2019/2 dated 30 December 2019. The views expressed in this article are those of the authors and do not necessarily reflect the Union's or the respective institutions' positions on the subject.

Institutional Review Board Statement: Not applicable.

Informed Consent Statement: Not applicable.

Data Availability Statement: All data generated or analyzed during this study are included in this published article.

Conflicts of Interest: The authors declare no conflict of interest.

Abbreviations

TQ	Thymoquinone
SLS	Sodium lauryl sulfate
SLG	Sodium lauroyl glutamate
Ph90	Phospholipon 90G
IVPT	In vitro permeation testing

References

1. Qureshi, K.A.; Imtiaz, M.; Al Nasr, I.; Koko, W.S.; Khan, T.A.; Jaremko, M.; Fatmi, M.Q. Antiprotozoal Activity of Thymoquinone (2-Isopropyl-5-methyl-1,4-benzoquinone) for the Treatment of Leishmania Major-Induced Leishmaniasis: In Silico and In Vitro Studies. *Antibiotics* **2022**, *11*, 1206. [CrossRef] [PubMed]
2. Ahmad, A.; Husain, A.; Mujeeb, M.; Alam Khan, S.; Najmi, A.K.; Siddique, N.A.; Damanhouri, Z.A.; Anwar, F. A review on therapeutic potential of Nigella sativa: A miracle herb. *Asian Pac. J. Trop. Biomed.* **2013**, *3*, 337–352. [CrossRef] [PubMed]
3. Chaieb, K.; Kouidhi, B.; Jrah, H.; Mahdouani, K.; Bakhrouf, A. Antibacterial activity of Thymoquinone, an active principle of Nigella sativa and its potency to prevent bacterial biofilm formation. *BMC Complement. Altern. Med.* **2011**, *11*, 29. [CrossRef] [PubMed]
4. Kohandel, Z.; Farkhondeh, T.; Aschner, M.; Samarghandian, S. Anti-inflammatory effects of thymoquinone and its protective effects against several diseases. *Biomed. Pharmacother.* **2021**, *138*, 111492. [CrossRef]
5. Isaev, N.K.; Genrikhs, E.E.; Stelmashook, E.V. Antioxidant Thymoquinone and Its Potential in the Treatment of Neurological Diseases. *Antioxidants* **2023**, *12*, 433. [CrossRef]
6. Salama, B.; Alzahrani, K.J.; Alghamdi, K.S.; Al-Amer, O.; Hassan, K.E.; Elhefny, M.A.; Albarakati, A.J.A.; Alharthi, F.; Althagafi, H.A.; Al Sberi, H.; et al. Silver Nanoparticles Enhance Oxidative Stress, Inflammation, and Apoptosis in Liver and Kidney Tissues: Potential Protective Role of Thymoquinone. *Biol. Trace Element Res.* **2023**, *201*, 2942–2954. [CrossRef] [PubMed]
7. Ghorbanibirgani, A.; Khalili, A.; Rokhafrooz, D. Comparing Nigella sativa Oil and Fish Oil in Treatment of Vitiligo. *Iran. Red Crescent Med. J.* **2014**, *16*, e4515. [CrossRef] [PubMed]
8. Hwang, J.R.; Cartron, A.M.; Khachemoune, A. A review of Nigella sativa plant-based therapy in dermatology. *Int. J. Dermatol.* **2021**, *60*, e493–e499. [CrossRef] [PubMed]
9. Sakib, R.; Caruso, F.; Aktar, S.; Belli, S.; Kaur, S.; Hernandez, M.; Rossi, M. Antioxidant Properties of Thymoquinone, Thymohydroquinone and Black Cumin (*Nigella sativa* L.) Seed Oil: Scavenging of Superoxide Radical Studied Using Cyclic Voltammetry, DFT and Single Crystal X-ray Diffraction. *Antioxidants* **2023**, *12*, 607. [CrossRef] [PubMed]
10. Badary, O.A.; Taha, R.A.; El-Din, A.M.G.; Abdel-Wahab, M.H. Thymoquinone Is a Potent Superoxide Anion Scavenger. *Drug Chem. Toxicol.* **2003**, *26*, 87–98. [CrossRef] [PubMed]
11. Mansour, M.A.; Nagi, M.N.; El-Khatib, A.S.; Al-Bekairi, A.M. Effects of thymoquinone on antioxidant enzyme activities, lipid peroxidation and DT-diaphorase in different tissues of mice: A possible mechanism of action. *Cell Biochem. Funct.* **2002**, *20*, 143–151. [CrossRef] [PubMed]
12. Algahtani, M.S.; Ahmad, M.Z.; Shaikh, I.A.; Abdel-Wahab, B.A.; Nourein, I.H.; Ahmad, J. Thymoquinone Loaded Topical Nanoemulgel for Wound Healing: Formulation Design and In-Vivo Evaluation. *Molecules* **2021**, *26*, 3863. [CrossRef] [PubMed]
13. Bhattacharya, S.; Ahir, M.; Patra, P.; Mukherjee, S.; Ghosh, S.; Mazumdar, M.; Chattopadhyay, S.; Das, T.; Chattopadhyay, D.; Adhikary, A. PEGylated-thymoquinone-nanoparticle mediated retardation of breast cancer cell migration by deregulation of cytoskeletal actin polymerization through miR-34a. *Biomaterials* **2015**, *51*, 91–107. [CrossRef] [PubMed]
14. Moghaddam, B.; Ali, M.H.; Wilkhu, J.; Kirby, D.J.; Mohammed, A.R.; Zheng, Q.; Perrie, Y. The application of monolayer studies in the understanding of liposomal formulations. *Int. J. Pharm.* **2011**, *417*, 235–244. [CrossRef] [PubMed]
15. Negi, P.; Sharma, I.; Hemrajani, C.; Rathore, C.; Bisht, A.; Raza, K.; Katare, O.P. Thymoquinone-loaded lipid vesicles: A promising nanomedicine for psoriasis. *BMC Complement. Altern. Med.* **2019**, *19*, 334. [CrossRef] [PubMed]
16. Sguizzato, M.; Ferrara, F.; Hallan, S.S.; Baldisserotto, A.; Drechsler, M.; Malatesta, M.; Costanzo, M.; Cortesi, R.; Puglia, C.; Valacchi, G.; et al. Ethosomes and Transethosomes for Mangiferin Transdermal Delivery. *Antioxidants* **2021**, *10*, 768. [CrossRef] [PubMed]
17. Matharoo, N.; Mohd, H.; Michniak-Kohn, B. Transferosomes as a transdermal drug delivery system: Dermal kinetics and recent developments. *Wiley Interdiscip. Rev. Nanomed. Nanobiotechnol.* **2023**, *16*, e1918. [CrossRef] [PubMed]
18. Ashtikar, M.; Nagarsekar, K.; Fahr, A. Transdermal delivery from liposomal formulations—Evolution of the technology over the last three decades. *J. Control. Release* **2016**, *242*, 126–140. [CrossRef] [PubMed]
19. Verma, P.; Pathak, K. Therapeutic and cosmeceutical potential of ethosomes: An overview. *J. Adv. Pharm. Technol. Res.* **2010**, *1*, 274–282. [CrossRef] [PubMed]
20. Gupta, R.; Kumar, A. Transfersomes: The Ultra-Deformable Carrier System for Non-Invasive Delivery of Drug. *Curr. Drug Deliv.* **2021**, *18*, 408–420. [CrossRef] [PubMed]
21. Grossi, L.N.; Braz, W.R.; da Silva, N.P.; Cazarim, E.L.C.C.; Palmieri, M.G.S.; Tavares, G.D.; Pittella, F. Ethosomes as delivery system for treatment of melanoma: A mini-review. *Oncologie* **2023**, *25*, 455–459. [CrossRef]

22. Das, S.K.; Chakraborty, S.; Roy, C.; Rajabalaya, R.; Mohaimin, A.W.; Khanam, J.; Nanda, A.; David, S.R. Ethosomes as Novel Vesicular Carrier: An Overview of the Principle, Preparation and its Applications. *Curr. Drug Deliv.* **2018**, *15*, 795–817. [CrossRef] [PubMed]
23. Lazaridis, N.; Alexopoulos, A.; Chatzi, E.; Kiparissides, C. Steric stabilization in emulsion polymerization using oligomeric nonionic surfactants. *Chem. Eng. Sci.* **1999**, *54*, 3251–3261. [CrossRef]
24. Elsayed, M.M.; Abdallah, O.Y.; Naggar, V.F.; Khalafallah, N.M. Deformable liposomes and ethosomes: Mechanism of enhanced skin delivery. *Int. J. Pharm.* **2006**, *322*, 60–66. [CrossRef] [PubMed]
25. Raj, A.; Dua, K.; Nair, R.S.; Chandran, C.S.; Alex, A.T. Transethosome: An ultra-deformable ethanolic vesicle for enhanced transdermal drug delivery. *Chem. Phys. Lipids* **2023**, *255*, 105315. [CrossRef] [PubMed]
26. Zhang, W.; Gao, Z.; Zhu, H.; Zhang, Q. Mixed micellization of cationic/anionic amino acid surfactants: Synergistic effect of sodium lauroyl glutamate and alkyl tri-methyl ammonium chloride. *J. Dispers. Sci. Technol.* **2022**, *43*, 2227–2239. [CrossRef]
27. Zhao, S.; Yang, X.; Garamus, V.M.; Handge, U.A.; Bérengère, L.; Zhao, L.; Salamon, G.; Willumeit, R.; Zou, A.; Fan, S. Mixture of Nonionic/Ionic Surfactants for the Formulation of Nanostructured Lipid Carriers: Effects on Physical Properties. *Langmuir* **2014**, *30*, 6920–6928. [CrossRef] [PubMed]
28. Vatanparast, H.; Shahabi, F.; Bahramian, A.; Javadi, A.; Miller, R. The Role of Electrostatic Repulsion on Increasing Surface Activity of Anionic Surfactants in the Presence of Hydrophilic Silica Nanoparticles. *Sci. Rep.* **2018**, *8*, 7251. [CrossRef] [PubMed]
29. Rojewska, M.; Smułek, W.; Grzywaczyk, A.; Kaczorek, E.; Prochaska, K. Study of Interactions between Saponin Biosurfactant and Model Biological Membranes: Phospholipid Monolayers and Liposomes. *Molecules* **2023**, *28*, 1965. [CrossRef] [PubMed]
30. Szczes, A.; Jurak, M.; Chibowski, E. Stability of binary model membranes-Prediction of the liposome stability by the Langmuir monolayer study (vol 372, pg 212, 2012). *J. Colloid Interface Sci.* **2014**, *435*, 199. [CrossRef]
31. Yang, L.; Wu, L.; Wu, D.; Shi, D.; Wang, T.; Zhu, X. Mechanism of transdermal permeation promotion of lipophilic drugs by ethosomes. *Int. J. Nanomed.* **2017**, *12*, 3357–3364. [CrossRef] [PubMed]
32. Duangjit, S.; Obata, Y.; Sano, H.; Onuki, Y.; Opanasopit, P.; Ngawhirunpat, T.; Miyoshi, T.; Kato, S.; Takayama, K. Comparative Study of Novel Ultradeformable Liposomes: Menthosomes, Transfersomes and Liposomes for Enhancing Skin Permeation of Meloxicam. *Biol. Pharm. Bull.* **2014**, *37*, 239–247. [CrossRef] [PubMed]
33. Abdellatif, M.M.; Khalil, I.A.; Khalil, M.A. Sertaconazole nitrate loaded nanovesicular systems for targeting skin fungal infection: In-vitro, ex-vivo and in-vivo evaluation. *Int. J. Pharm.* **2017**, *527*, 1–11. [CrossRef] [PubMed]
34. Haq, A.; Michniak-Kohn, B. Effects of solvents and penetration enhancers on transdermal delivery of thymoquinone: Permeability and skin deposition study. *Drug Deliv.* **2018**, *25*, 1943–1949. [CrossRef] [PubMed]
35. Virani, A.; Puri, V.; Mohd, H.; Michniak-Kohn, B. Effect of Penetration Enhancers on Transdermal Delivery of Oxcarbazepine, an Antiepileptic Drug Using Microemulsions. *Pharmaceutics* **2023**, *15*, 183. [CrossRef] [PubMed]
36. Virani, A.; Dholaria, N.; Mohd, H.; Albayati, N.; Michniak-Kohn, B. Effect of chemical penetration enhancers on the transdermal delivery of olanzapine in human skin in vitro. *AAPS Open* **2024**, *10*, 4. [CrossRef]
37. Dvořáková, K.; Štěpánek, P.; Kroupová, J.; Zbytovská, J. *N*-Alkylmorpholines: Potent Dermal and Transdermal Skin Permeation Enhancers. *Pharmaceutics* **2021**, *14*, 64. [CrossRef] [PubMed]
38. Virani, A.; Dholaria, N.; Matharoo, N.; Michniak-Kohn, B. A Study of Microemulsion Systems for Transdermal Delivery of Risperidone Using Penetration Enhancers. *J. Pharm. Sci.* **2023**, *112*, 3109–3119. [CrossRef] [PubMed]
39. Dopierała, K.; Syguda, A.; Wojcieszak, M.; Materna, K. Effect of 1-alkyl-1-methylpiperidinium bromides on lipids of fungal plasma membrane and lung surfactant. *Chem. Phys. Lipids* **2022**, *248*, 105240. [CrossRef]
40. Khattari, Z.; Langer, U.; Aliaskarisohi, S.; Ray, A.; Fischer, T. Effects of soluble surfactants on the Langmuir monolayers compressibility: A comparative study using interfacial isotherms and fluorescence microscopy. *Mater. Sci. Eng. C* **2011**, *31*, 1711–1715. [CrossRef]
41. McConlogue, C.W.; Malamud, D.; Vanderlick, T. Interaction of DPPC monolayers with soluble surfactants: Electrostatic effects of membrane perturbants. *Biochim. Biophys. Acta (BBA)-Biomembr.* **1998**, *1372*, 124–134. [CrossRef]
42. Balata, G.F.; Faisal, M.M.; Elghamry, H.A.; Sabry, S.A. Preparation and Characterization of Ivabradine HCl Transfersomes for Enhanced Transdermal Delivery. *J. Drug Deliv. Sci. Technol.* **2020**, *60*, 101921. [CrossRef]
43. González-Rodríguez, M.L.; Arroyo, C.M.; Cózar-Bernal, M.J.; González-R, P.L.; León, J.M.; Calle, M.; Canca, D.; Rabasco, A.M. Deformability properties of timolol-loaded transfersomes based on the extrusion mechanism. Statistical optimization of the process. *Drug Dev. Ind. Pharm.* **2016**, *42*, 1683–1694. [CrossRef] [PubMed]
44. Zhang, Z.J.; Osmałek, T.; Michniak-Kohn, B. Deformable Liposomal Hydrogel for Dermal and Transdermal Delivery of Meloxicam. *Int. J. Nanomed.* **2020**, *15*, 9319–9335. [CrossRef] [PubMed]
45. Ban, E.; Park, M.; Jeong, S.; Kwon, T.; Kim, E.-H.; Jung, K.; Kim, A. Poloxamer-Based Thermoreversible Gel for Topical Delivery of Emodin: Influence of P407 and P188 on Solubility of Emodin and Its Application in Cellular Activity Screening. *Molecules* **2017**, *22*, 246. [CrossRef] [PubMed]
46. Song, C.K.; Balakrishnan, P.; Shim, C.K.; Chung, S.J.; Chong, S.; Kim, D.D. A novel vesicular carrier, transethosome, for enhanced skin delivery of voriconazole: Characterization and in vitro/in vivo evaluation. *Colloids Surf. B Biointerfaces* **2012**, *92*, 299–304. [CrossRef] [PubMed]

47. El Zaafarany, G.M.; Awad, G.A.S.; Holayel, S.M.; Mortada, N.D. Role of edge activators and surface charge in developing ultradeformable vesicles with enhanced skin delivery. *Int. J. Pharm.* **2010**, *397*, 164–172. [CrossRef] [PubMed]
48. Nikolic, P.; Mudgil, P. The Cell Wall, Cell Membrane and Virulence Factors of *Staphylococcus aureus* and Their Role in Antibiotic Resistance. *Microorganisms* **2023**, *11*, 259. [CrossRef] [PubMed]

Disclaimer/Publisher's Note: The statements, opinions and data contained in all publications are solely those of the individual author(s) and contributor(s) and not of MDPI and/or the editor(s). MDPI and/or the editor(s) disclaim responsibility for any injury to people or property resulting from any ideas, methods, instructions or products referred to in the content.